Supporting Information

AIEgens for Dual Second Harmonic Generation and Fluorescence "Turn-On" Imaging of Membrane and Photodynamic Therapy in Cancer Cells

Yingying Peng,[a] Yang Yan,[b] Peng Li,[c] Bifei Li, [a] Hanlin Jiang,[a] Bing Guo,[a] Qunhui Yuan, [d*] Wei Gan[a*]*

Dr. Y. Peng, Dr. Y. Yan, Dr. B. Li, H. Jiang, Prof. Dr. B. Guo, Prof. Dr. W. Gan

Shenzhen Key Laboratory of Flexible Printed Electronics Technology, and School of Science, Harbin Institute of Technology (Shenzhen), University Town, Shenzhen 518055, Guangdong; School of Chemistry and Chemical Engineering, Harbin Institute of Technology, Harbin 150001, Heilongjiang, China

Email: guobing2020@hit.edu.cn, ganwei@hit.edu.cn

Dr. Y. Yan

Institute of Urology, The Third Affiliated Hospital of Shenzhen University, Youyi Road, Luohu District, Shenzhen 518000, Guangdong China

P. Li

School of Life and Health Sciences, The Chinese University of Hong Kong (Shenzhen), Longxiang Road, Longgang District, Shenzhen 518172, Guangdong China

Prof. Dr. Q. Yuan

Shenzhen Key Laboratory of Flexible Printed Electronics Technology, and School of Materials Science and Engineering, Harbin Institute of Technology (Shenzhen), University Town, Shenzhen 518055, Guangdong, China

Email: yuanqunhui@hit.edu.cn

# Contents

1. Reagents and materials

Bis (4-(diethylamino) phenyl) methanone, isonicotinaldehyde, iodoethane, 1-iodohexane, 1-iodo-decane, titanium tetrachloride, K_2CO_3, Zn, Na_2SO_4, dichloromethane (DCM), petroleum ether (PE), ethyl acetate (EA), N, N-dimethylformamide (DMF), tetrahydrofuran (THF), dimethylsulfoxide (DMSO), methylthiazolyldiphenyl-tetrazolium bromide (MTT), Calcein/PI cell viability/Cytotoxicity assay kit, Mito-tracker green, 3,3′-dioctadecyloxacarbocyanine perchlorate (DIO), bisbenzimide H 33342 (Hoechst 33342), 9, 10-anthracenedipropanoic acid (ABDA), methyl blue (MB) and rose bengal (RB) were purchased from Sigma-Aldrich. Dulbecco`s modified essential medium (DMEM), Fetal bovine serum (FBS), Streptomycin-penicillin and phosphate buffer saline (PBS) were purchased from Gibco (Life Technologies). Deionized water (18.2 MΩ·cm) was purified with a water purification system (WP-UP-UV-20) from Sichuan Water Technology Development Co. Ltd (Chengdu, China).

2. Cell cultivation

K562 (Human chronic myelogenous leukemia), Hela (America Type Culture Collection) and U87MG (Human glioblastoma) cells were stabilized in a DMEM containing 10% FBS and 1% (both v/v ratio) penicillin (100 units/mL)-streptomycin (100 μg/mL) with a humidified 5% CO_2 incubator at 37℃.

3. Synthesis, NMR and ESI-MS of EAPVs

^{1}HNMR and ^{13}CNMR were collected with a Bruker AV-400 spectrometer. The ESI-MS spectra were obtained using LTQ Orbit rap XL instruments. The synthetic routes and structural characterization for **EAPV**s is shown in Scheme S1 and Figure S1-12.
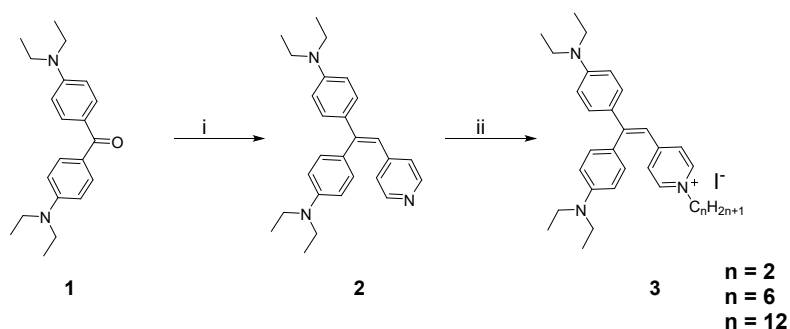
Scheme S1. Synthetic routes of **EAPVs**. Reagents and condition: (i) Isonicotinaldehyde, Zn, TiCl$_4$, THF, N$_2$, 70°C, reflux, 24 h. (ii) Iodoethane for **EAPV2**/1-iodohexane for **EAPV6**/1-iododo-decane for **EAPV12**, DMF, 80°C, reflux, 24 h.

Synthesis of 4,4'-(2-(pyridin-4-yl) ethene-1,1-diyl) bis (N, N-diethylaniline) (**Compound 2**). Bis (4-(diethylamino) phenyl) methanone (compound 1, 5 g, 15.41 mM), isonicotinaldehyde (1.45 mL, 15.41 mM) and Zn (12.0 g, 183.54 mM) were dissolved in THF (30 mL) and stirred under nitrogen at 0 °C. TiCl$_4$ (10.0 mL, 91.0 mM) was added dropwise over a period of 30 min. Then, the ice-water-bath was removed and the mixture was stirred for 12 h at 70 °C. After cooling down to room temperature, the resulting mixture was quenched by saturated K$_2$CO$_3$ solution (10 mL) and extracted with DCM, the organic fraction was combined and washed with brine, dried over Na$_2$SO$_4$, followed with evaporation under reduced pressure and purification with silica gel column chromatography using PE/ EA (v/v, 20 :1) as the eluent to provide the desired products as yellow oil (3.97 g, 65 %). ^{1}H NMR (400 MHz, CDCl$_3$) δ 8.32 (d, J = 6.1 Hz, 2H), 7.28 (d, J = 9.1 Hz, 2H), 7.04 (d, J = 8.8 Hz, 2H), 6.93 (d, J = 6.1 Hz, 2H), 6.63 (dd, J = 18.0, 8.8 Hz, 5H), 3.41 (qd, J = 7.0, 3.8 Hz, 8H), 1.27-1.18 (m, 13H). ^{13}C NMR (101 MHz, CDCl3) δ 149.23 (s), 147.95 (d, J = 16.6 Hz), 147.63 (s), 146.60 (s), 131.52 (s), 129.96 (s), 129.45 (s), 126.14 (s), 123.63 (s), 119.76 (s), 111.53 (s), 110.97 (s), 44.32 (s), 12.64 (s). ESI (m/z): calculated for C$_{27}$H$_{33}$N$_3$ 422.2566, found 422.2561.

Synthesis of 4-(2,2-bis(4-(diethylamino) phenyl) vinyl)-1-ethylpyridin-1-ium (**EAPV2**). The mixture of compound 2 (1 g, 2.50 mmol) and iodoethane (0.60 mL, 7.51 mmol) was dissolved

in 10 mL dried DMF and stirred overnight under nitrogen at 90 ℃. After cooling down to room temperature, the solvent was removed under reduced pressure using rotary evaporator. Then, the resulting crude products was recrystallized by the mixture of DCM and diethyl ether to obtained pure **EAPV2** as red solid (0.87 g, 81%). ^{1}H NMR (400 MHz, CDCl$_3$) δ 8.49 (s, 2H), 7.32 (d, J = 8.6 Hz, 2H), 7.28 (d, J = 3.0 Hz, 2H), 7.06 (d, J = 8.6 Hz, 2H), 6.75 – 6.58 (m, 5H), 4.70 (d, J = 5.3 Hz, 2H), 3.65 – 3.30 (m, 8H), 1.64 (d, J = 9.9 Hz, 4H), 1.24 (t, J = 7.1 Hz, 12H). ^{13}C NMR (101 MHz, DMSO) δ 156.62 (s), 154.61 (s), 149.48 (s), 148.84 (s), 142.90 (s), 131.64 (s), 131.04 (s), 127.53 (s), 125.17 (s), 124.07 (s), 116.06 (s), 112.03 (s), 111.38 (s), 54.82 (s), 44.25 (s), 16.44 (s), 12.94 (s) . ESI (m/z): calculated for C$_{29}$H$_{38}$N$_3{}^+$, [M+H]$^+$ 429.3134, found 429.3134.

Synthesis of 4-(2,2-bis (4-(diethylamino) phenyl) vinyl)-1-hexylpyridin-1-ium (**EAPV6**). **EAPV6** was synthesized according to the similar synthetic procedure described in **EAPV2** by using 1-iodohexane to afford **EAPV6** as red solid (yield: 86%). ^{1}H NMR (400 MHz, CDCl$_3$) δ 8.45 (d, J = 6.7 Hz, 2H), 7.32 (d, J = 8.9 Hz, 2H), 7.27 (d, J = 6.7 Hz, 2H), 7.05 (d, J = 8.3 Hz, 2H), 6.74 – 6.59 (m, 5H), 4.62 (t, J = 7.3 Hz, 2H), 3.45 (dd, J = 14.0, 7.0 Hz, 9H), 1.99 – 1.91 (m, 2H), 1.64 (s, 6H), 1.25 (dd, J = 14.3, 7.1 Hz, 13H), 0.90 (t, J = 6.8 Hz, 4H). ^{13}C NMR (101 MHz, CDCl$_3$) δ 162.21 (s), 159.01 (s), 155.20 (s), 149.37 (s), 148.92 (s), 141.26 (s), 131.61 (s), 131.08 (s), 127.05 (s), 124.67 (s), 123.20 (s), 114.48 (s), 111.12 (s), 110.52 (s), 59.59 (s), 46.19 (s), 30.74 (s), 25.26 (s), 21.99 (s), 13.57 (s), 8.50 (s) . ESI (m/z): calculated for C$_{33}$H$_{46}$N$_3{}^+$, [M+H]$^+$ 485.3769found 485.3774.

Synthesis of 4-(2,2-bis(4-(diethylamino) phenyl) vinyl)-1-dodecylpyridin-1-ium (**EAPV12**). **EAPV12** was synthesized according to the similar synthetic procedure described in **EAPV2** by using 1-iododo-decane to afford **EAPV12** as red solid (yield: 71%). ^{1}H NMR (400 MHz, CDCl$_3$) δ 8.43 (d, J = 7.0 Hz, 2H), 7.28 (d, J = 9.0 Hz, 2H), 7.23 (d, J = 6.9 Hz, 2H), 7.02 (d, J = 8.8 Hz, 2H), 6.66 (s, 1H), 6.62 (dd, J = 12.2, 3.1 Hz, 4H), 4.59 (t, J = 7.3 Hz, 2H), 3.43 (dd,

$J = 14.1, 7.0$ Hz, 8H), 1.21 (dd, $J = 14.1, 7.0$ Hz, 31H), 0.87 (dd, $J = 7.9, 5.7$ Hz, 6H). ^{13}C NMR (101 MHz, CDCl$_3$) δ 159.02 (s), 155.46 (s), 149.67 (s), 149.28 (s), 141.90 (s), 131.99 (s), 131.40 (s), 127.60 (s), 125.11 (s), 122.90 (s), 115.09 (s), 111.54 (s), 110.91 (s), 60.04 (s), 44.50 (d, $J = 11.7$ Hz), 32.18-31.34 (m), 30.79-29.30 (m), 29.13 (s), 26.06 (s), 22.71 (s), 14.16 (s), 12.65 (s). ESI (m/z): calculated for $C_{39}H_{58}N_3^+$ [M+H]$^+$ 569.4695, found 569.4699.

4. UV-Vis and Fluorescence spectra

The UV-Vis absorption was recorded on a Shimadzu (Suzhou, china) UV-1800 spectrophotometer with a 1 cm quartz cuvette. The fluorescence spectra were measured in an F-7000 spectrophotometer (HATACHI, Japan).

5. Molar extinction coefficient Calculation.

The molar extinction coefficient (ε) for all EAPVs were determined based on Figure S13 with the Beer-Lambert Law:

$$A = \varepsilon l c$$

where A is the absorbance at 500 nm for the EAPV solutions, l represents optical path (1cm in this article), c indicates the concentration of the EAPV solutions.

6. ROS detection. In order to demonstrate the ROS generation efficiency of EAPVs, ABDA was used as indicator to achieve the ROS detection upon irradiation with a white light (50 mW cm^{-2}). The ABDA aqueous solution (100 µmol/L) was mixed with each EAPV solution (10 µmol/L) and exposed to the light with different irradiation time with the decomposition of ABDA monitored at 378 nm.

7. ROS quantum yield. The ROS quantum yield for all EAPVs (Φ_{sample}) were measured using ABDA as an indicator and Rose Bengal (RB) as a standard, respectively. It is known that the

ROS quantum yield of RB (Φ_{RB}) in water is 0.75 [1]. Then, the ROS quantum yield for all EAPVs were calculated through the following equation:

$$\Phi_{sample} = \frac{\Phi_{RB}(K_{sample} \cdot A_{RB})}{K_{RB} \cdot A_{sample}}$$

where K_{sample} and K_{RB} are the decomposition rate constants determined by the plot of ln (A_0/A) versus the irradiation time, in which A_0 and A indicate the initial ABDA absorbance and the ABDA absorbance at different irradiation time. A_{RB} and A_{sample} are the integration of the LED intensity in their respective absorbance bands between 400 nm and 700 nm.

8. Computation

Density Functional Theory (DFT) calculations based on B3LYP/6-311G (d, p) basis set were performed through Gaussian 09 program to optimize the molecular geometries and compute the molecular orbital levels. The first hyperpolarizability (β) for **EAPVs** were calculated in water based on Hartree-Fock (6-311G (d, p) basis set) with a wavelength of 810 nm and analyzed using Multiwfn.

9. SHG (also hyper-Rayleigh)/TPF spectral detection

The instrument for SHG (or hyper-Rayleigh in experiments without cells, in the following all referred as SHG) and TPF detection has been described in our previous work [2-3]. Briefly, we used a Ti-sapphire laser (MaiTai HP, Spectra Physics, pulse width ~100 fs, repetition rate 80 MHz, laser power 300 mW) with wavelength of 810 nm as excitation laser (Scheme S2). Initially, the incident beam passed through a high pass filter (FGL9, >720 nm, Thorlabs) and focused on the sample pool (cylindrical quartz container with 13 mm inner diameter). A magnetic stirrer was used to ensure efficient mixing of the cells and the dyes to avoid local heating effect. Then, the output signal at the forward direction was divided into the SHG beam and TPF beam by a dichroic mirror. The SHG signal at ~405 nm went through two bandpass

filters (FB405-10, 405/10 nm, Thorlabs) and was detected by a PMT (Hamamatsu R928). The TPF signal mainly at the wavelength range of 500-600 nm went through two bandpass filters (FBGB37S, 335-610 nm, Thorlabs) and was focused in a monochromator (Omni1509, Zolix Instruments Co., Ltd, China) and detected by a PMT (Hamamatsu R1527p). A preamplifier (SR445A, Stanford Research System) with an amplification factor of 5 and a single photon counter (SR400, Stanford Research) were used to amplify and analyze the obtained signals. The PMT voltage was set as -900 V.
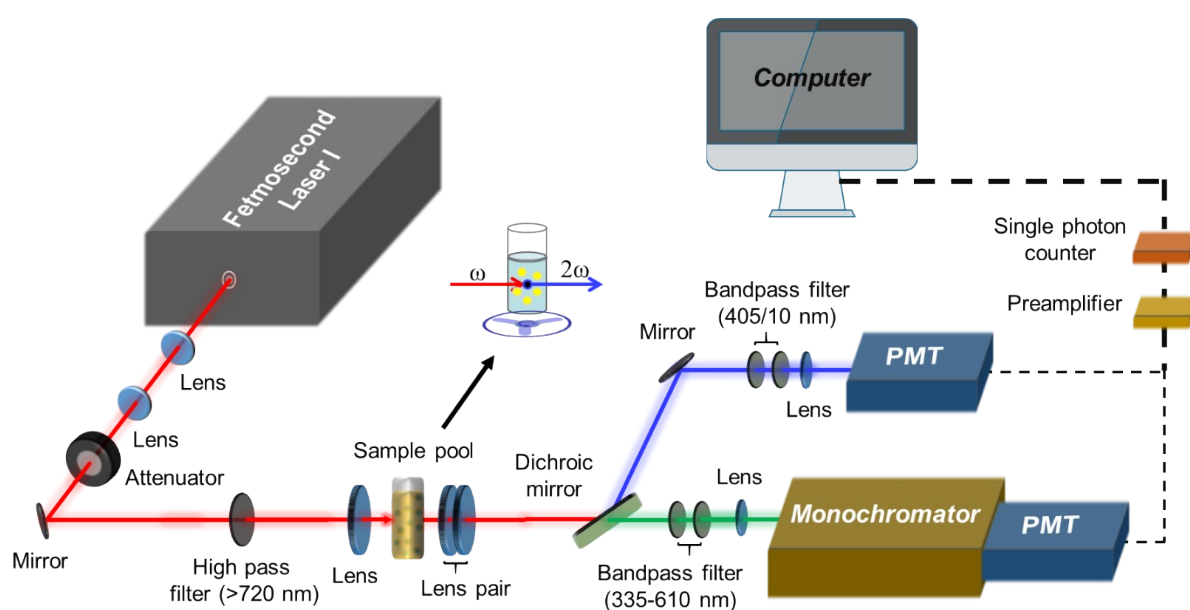
Scheme S2. Diagram of the setup for the detection of the SHG and TPF signals.

10. SHG imaging

A laser system from Light Conversion was utilizied as the light source (810 nm, 8 mw) for SHG imaging. A Yb doped solid state pulse amplifiers (Pharos) delivered 50 kHz, 1030 nm, 10 W, ~300 fs laser pulses to the optical parametric amplifier (ORPHEUS-HP) and generated 810 nm laser. As shown in Scheme S3, the laser was successively passed through a high pass filter (FGL9, >720 nm, Thorlabs) and a pair of lenses with the focal length of 15 cm. Then, a combination of halfwave plate (AHWP10M-980, Thorlabs) and polarizer (CCM1-PBS252,

Thorlabs) was used to control the beam power as 8 mw. After that, the laser was focused on the sample by a 4x objective lens (LWDPLF4x, 0.13 NA, Sunny optical technology) to get a relatively large focusing area for the illumination of a whole cell. The SHG image at the forward direction was collected by a 60x objective lens (UplanSApo, 1.35 NA, Olympus) and went across a bandpass filter (BG39, 330-610 nm, Thorlabs) to filter out the residual 810 nm light, a bandpass filter (405 ± 12 nm, Thorlabs) to get the SHG signal. Finally, the oputput signal was focused in a monochromator (ANDOR, KYMERA-328i, UK) and detected by an EMCCD camera (Andor iXon 888s).
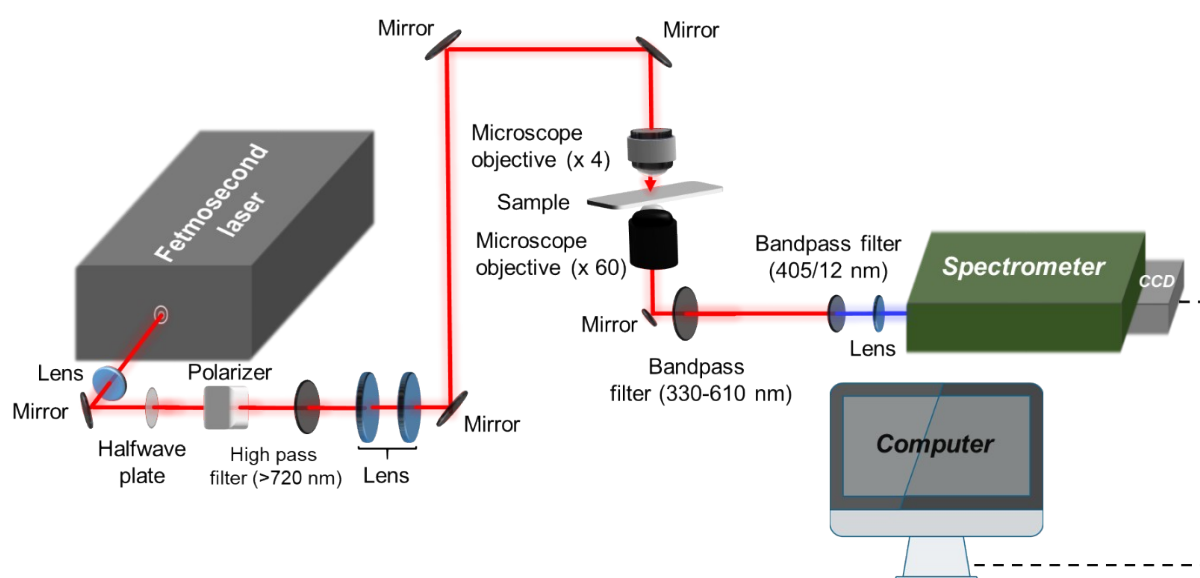
Scheme S3. Diagram of the setup for simultaneous detection of the SHG and TPF imaging.

11. In vitro confocal laser sacnning microscopy (CLSM)

The cell density used for CLSM (Leica TCS SP8 Scan Head) was $2*10^6$ in the 35 mm confocal dish. Before the imaging, the cells were successively incubated with 100 nM Mito-tracker/DIO and Hochest 33342 for 30 min, followed by rinses with PBS for three times. Then, the **EAPVs** solutions were slowly added into these chamber befote the CLSM imaging.

In the intracellular singlet oxygen imaging measurements, DCFH-DA (2,7-Dichloro-fluoresceindiacetate) was used as the intracellular singlet oxygen indicator. Berifly, the Hela

cells were incubated and plated onto the 35 mm confocal chamber for 24 h. Then, the cells were sequentially incubated with **EAPVs** (20 μM) and DCFH-DA (10 μM) for another 30 min, respectively. After that, the cells were exposed to white light (50 W/cm^2) with various lighting duration. The green fluorescence of DCFH-DA was captured through CLSM.

In the Live/dead cell co-staining assay, Hela cells were seeded in 35 mm confocal chamber with a density of 7*10^4 for 24 h. After that, the culture medium was placed with fresh medium containing 20 μM **EAPVs** to incubate for another 3 h. Then, the cells were irradiated under white light (50 W/cm^2) with different time, followed by the addition of calcein-AM (3 μM) and PI (4 μM) for 30 min, the cells were washed with PBS and immediately imaging using CLSM.

12. In vitro dark & light cytotoxicity

The cell viability was estimated by MTT assay. Initially, the Hela cells were seeded in 96-well plate with a density of 7*10^4 and incubated for 24 h. Then, the medium was replaced by fresh medium containing different concentration of **EAPVs** solution and the cells were cultured for another 24 h at 37℃. Then, the culture medium was discarded, followed by the addition of MTT solution with the concentration of 0.5 mg/mL for each sample. After 4 h incubation, the cells were irradiated with white light (50 W/cm^2, 20 min) and further incubated for 24 h at 37℃. Finally, the MTT solution was gently removed, 100 μM DMSO was added to dissolve the crystals. Then, the absorbance for each plate at 540 nm was measured through a Bio-Rad microplate reader. The cell viability was calculated by the following equation [4]:

$$Cell\ viability\ (\%) = \left(\frac{OD_{treated} - OD_{blank}}{OD_{control} - OD_{blank}}\right) * 100\ \%$$

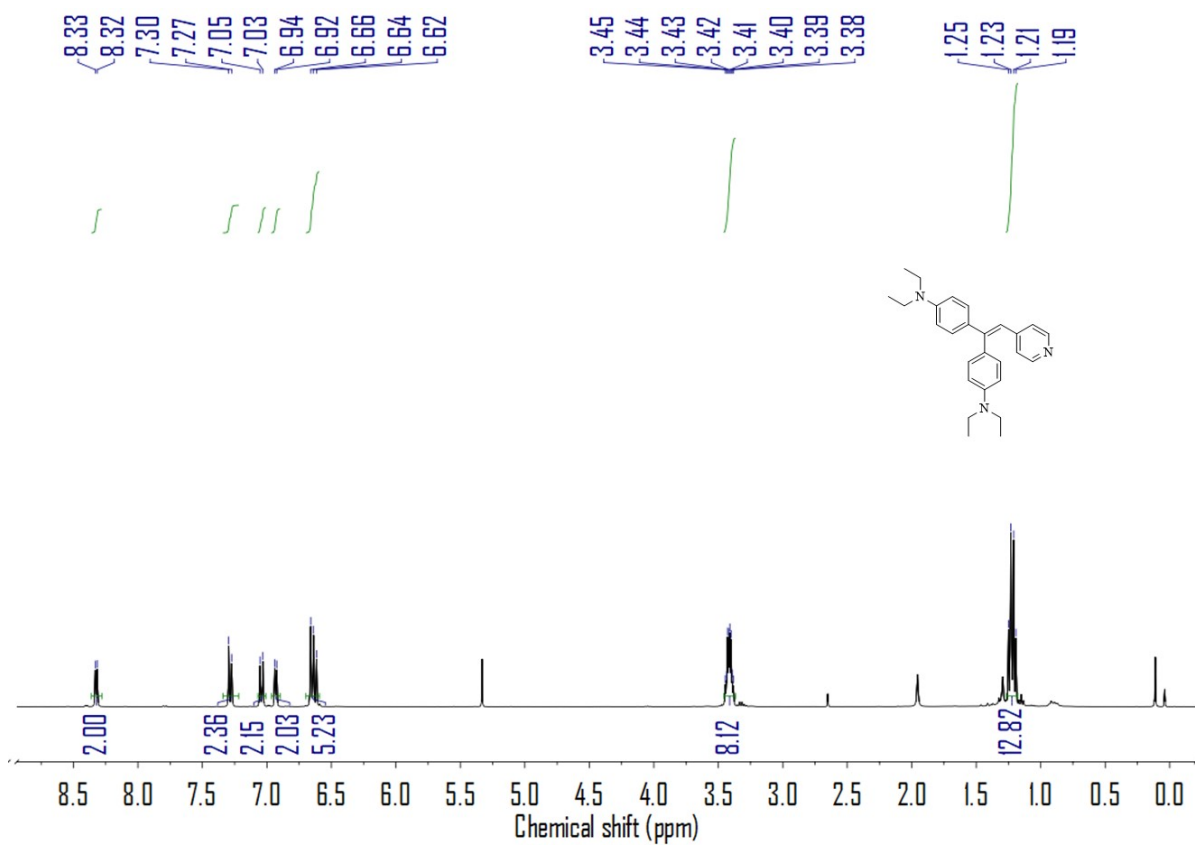For the dark cytotoxicity sample, the irradiating step was absent and rest part of the experiments unchanged.
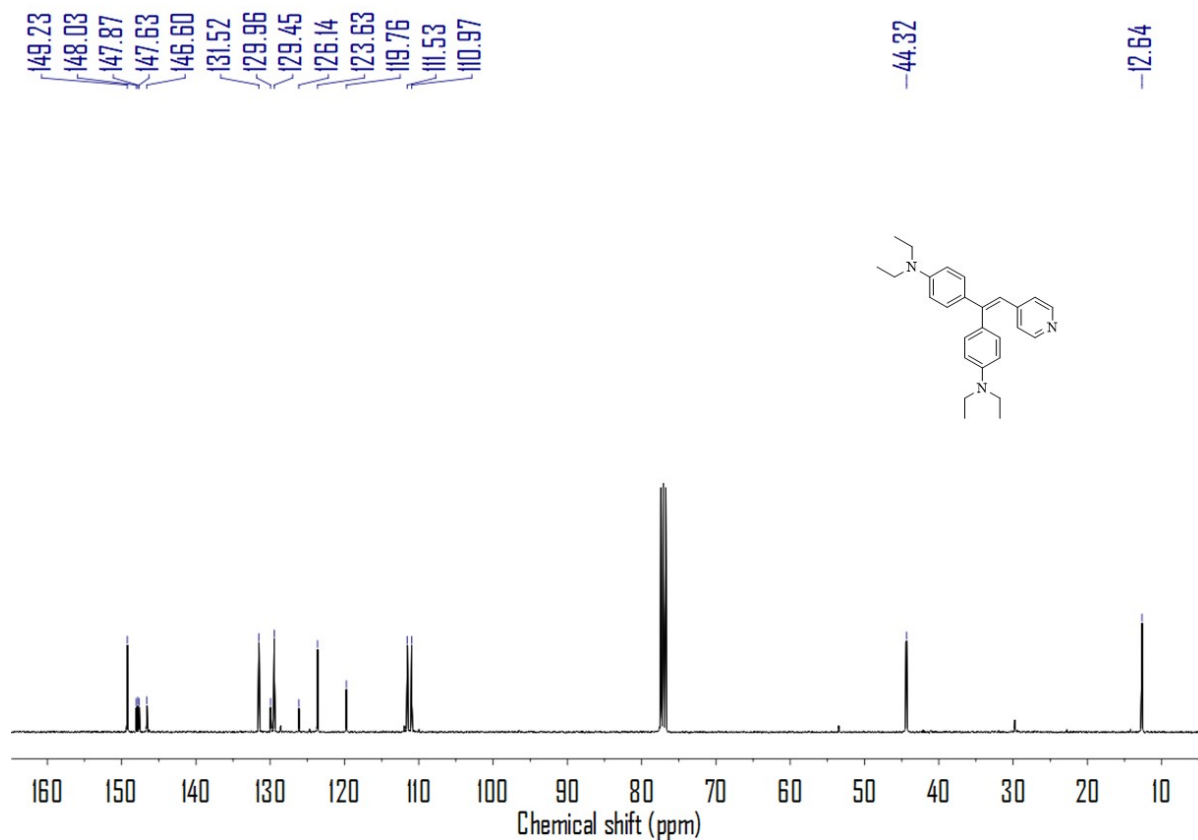
Figure S1. The ^{1}H NMR spectrum of compound **2**.

Figure S2. The ^{13}C NMR spectrum of compound **2**.
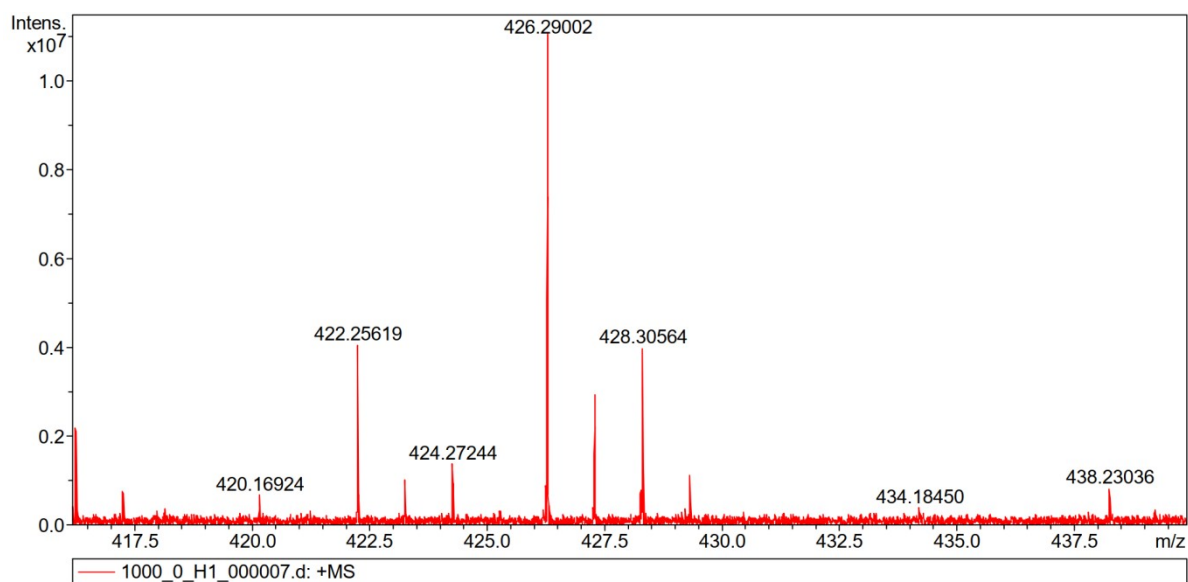

Figure S3. ESI-Mass spectrum of compound **2**.
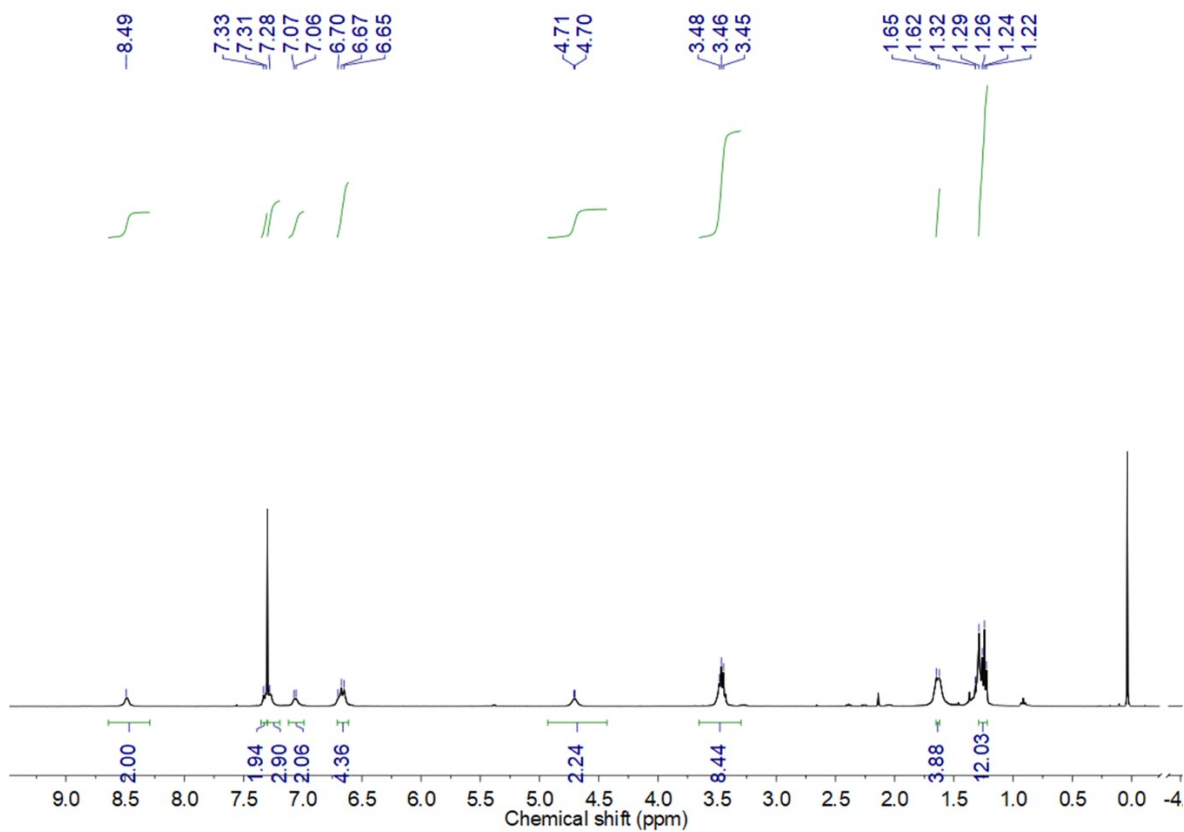
Figure S4. The ^{1}H NMR spectrum of **EAPV2**.
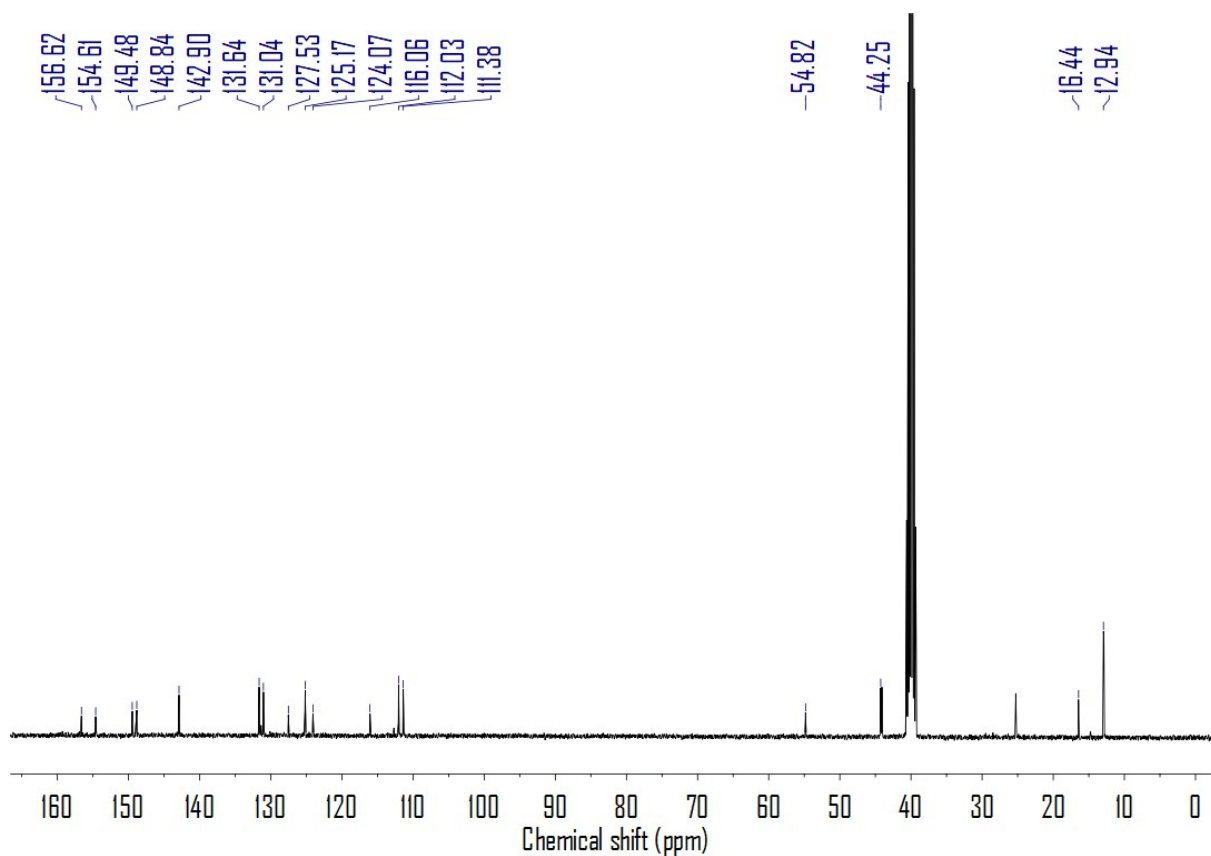
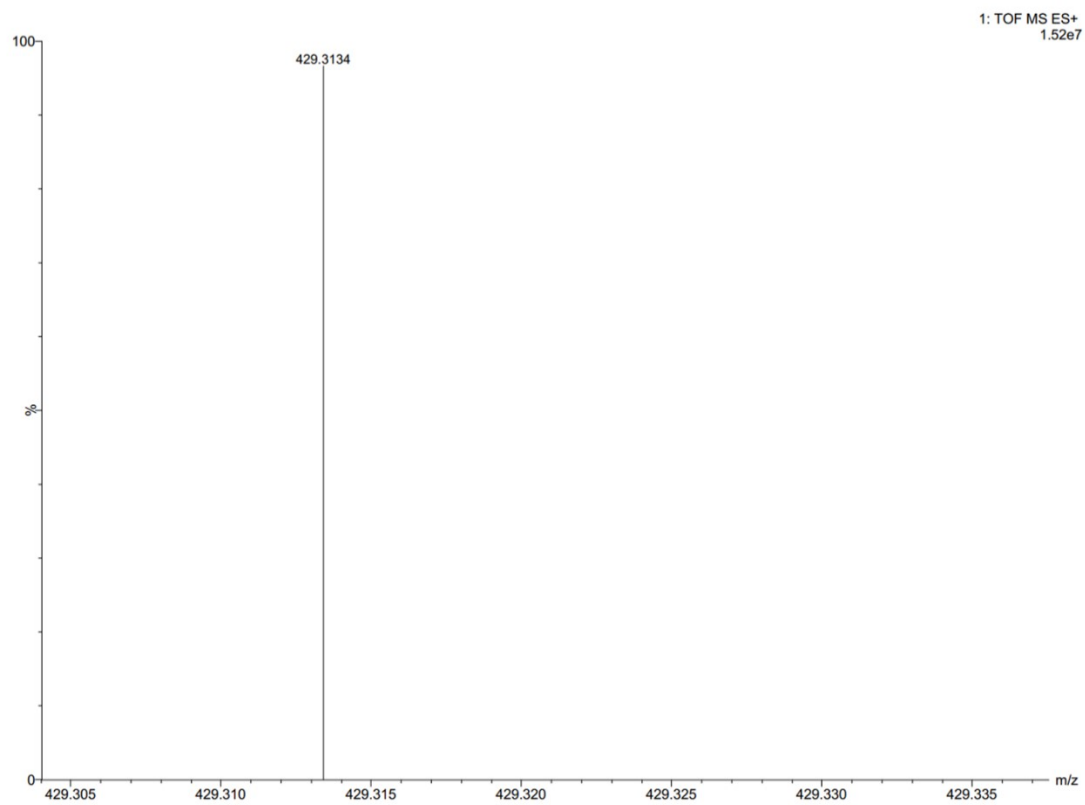**Figure S5.** The ^{13}C NMR spectrum of **EAPV2**.

1: TOF MS ES+
1.52e7

429.3134

Figure S6. ESI-Mass spectrum of **EAPV2**.
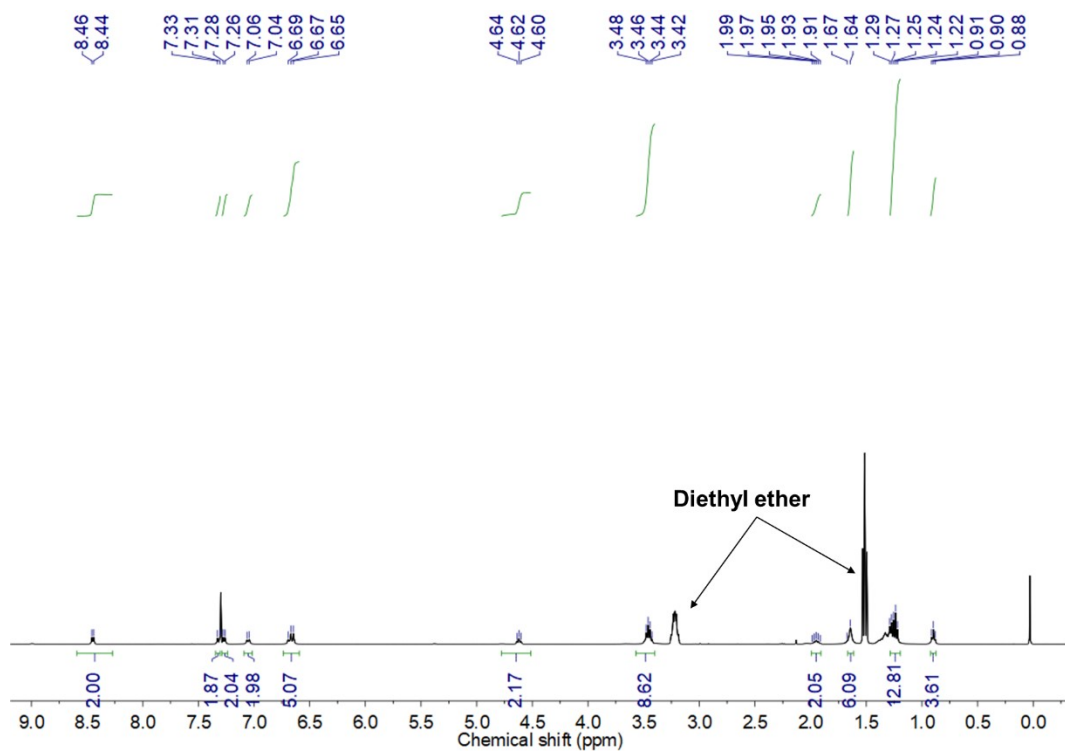
Figure S7. The ^{1}H NMR spectrum of **EAPV6**.
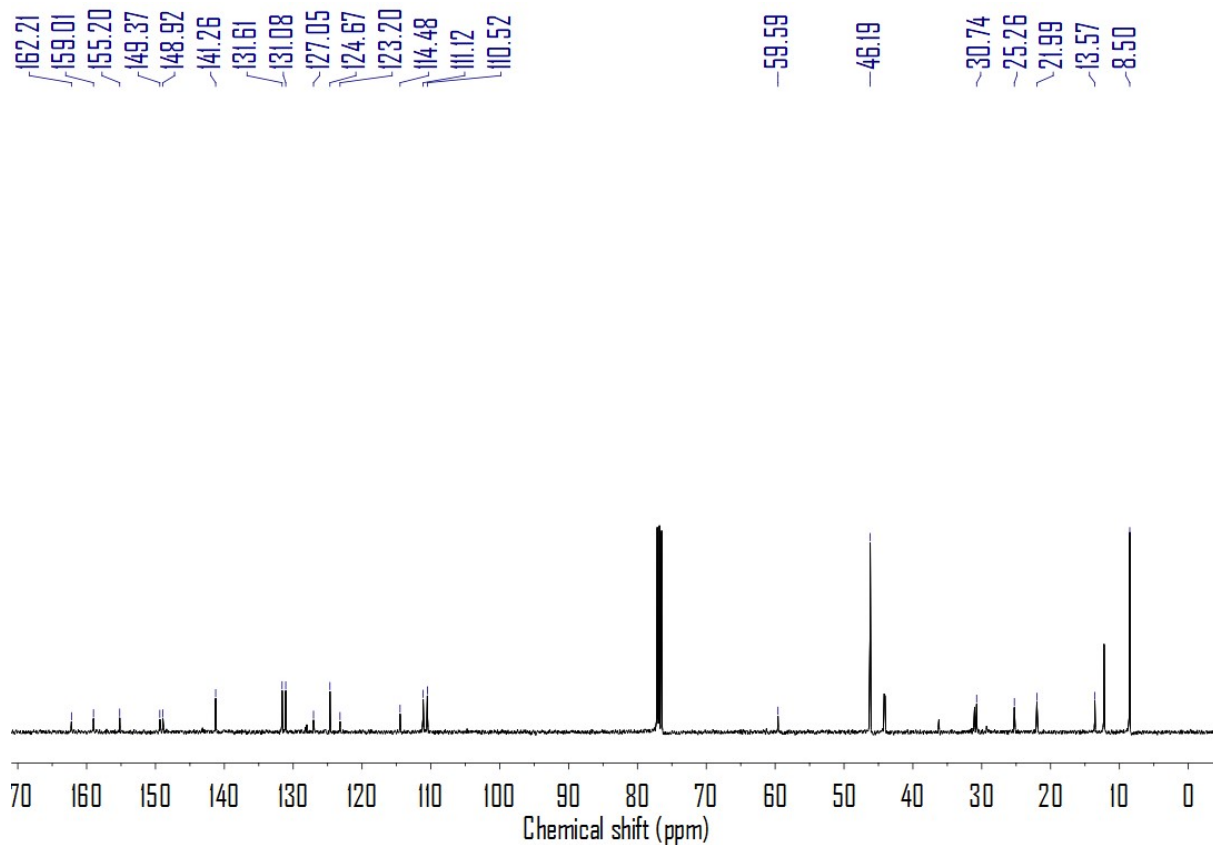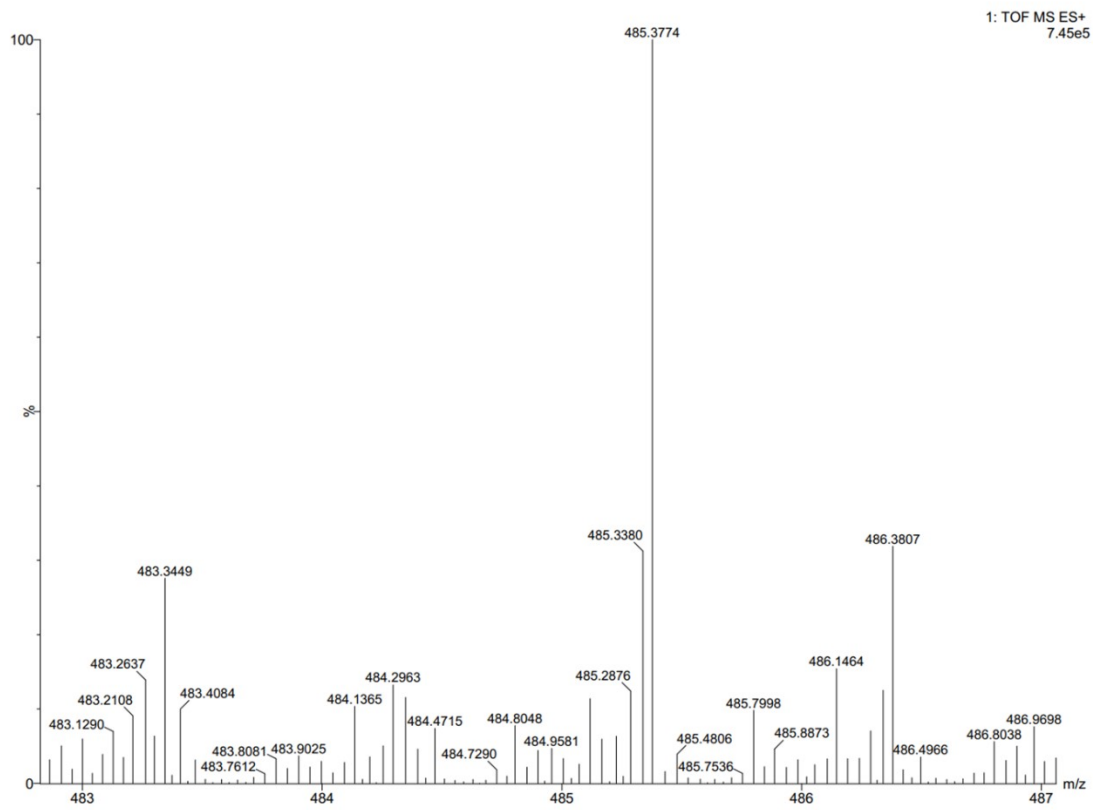
Figure S9. ESI-Mass spectrum of **EAPV6**.
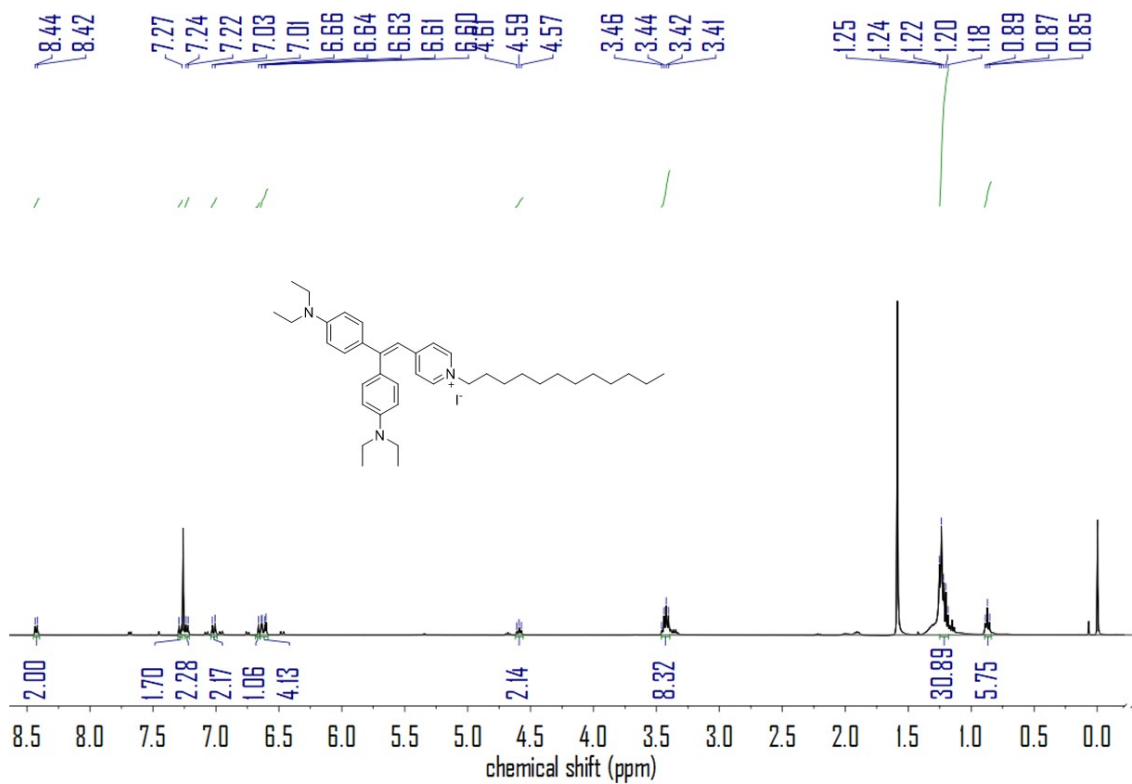
Figure S10. The ^{1}H NMR spectrum of **EAPV12**.
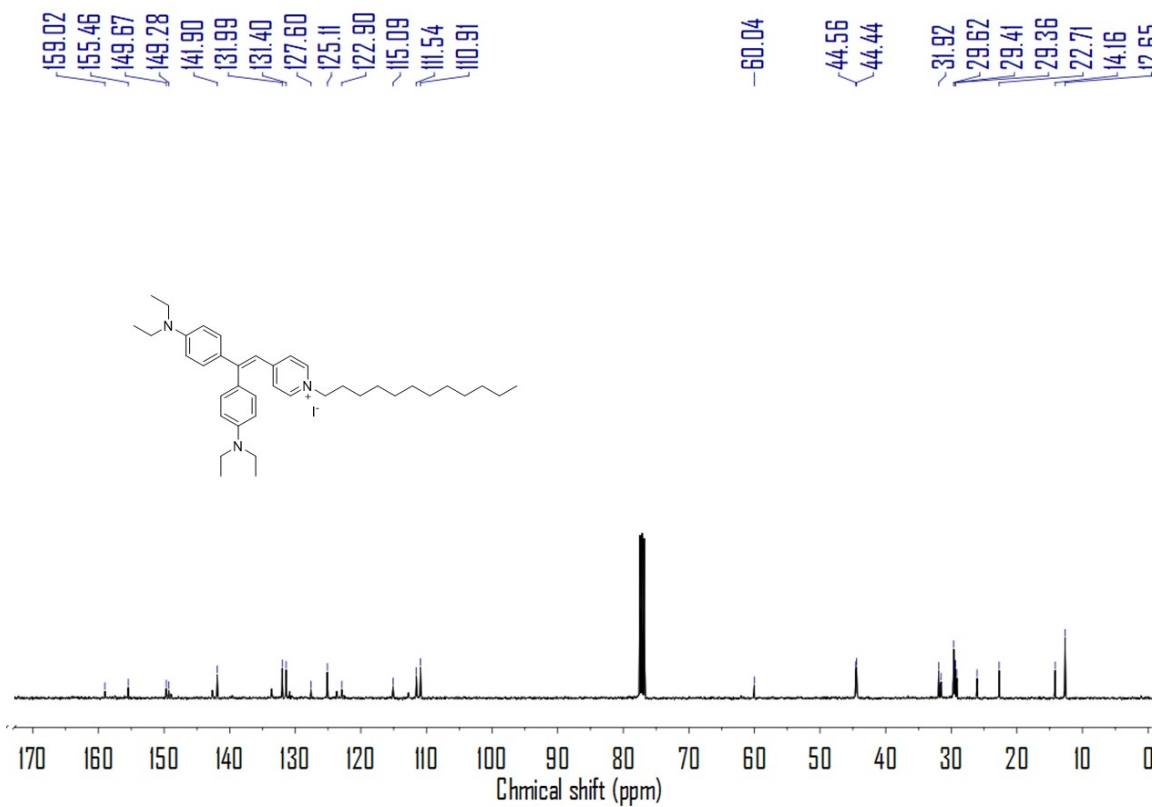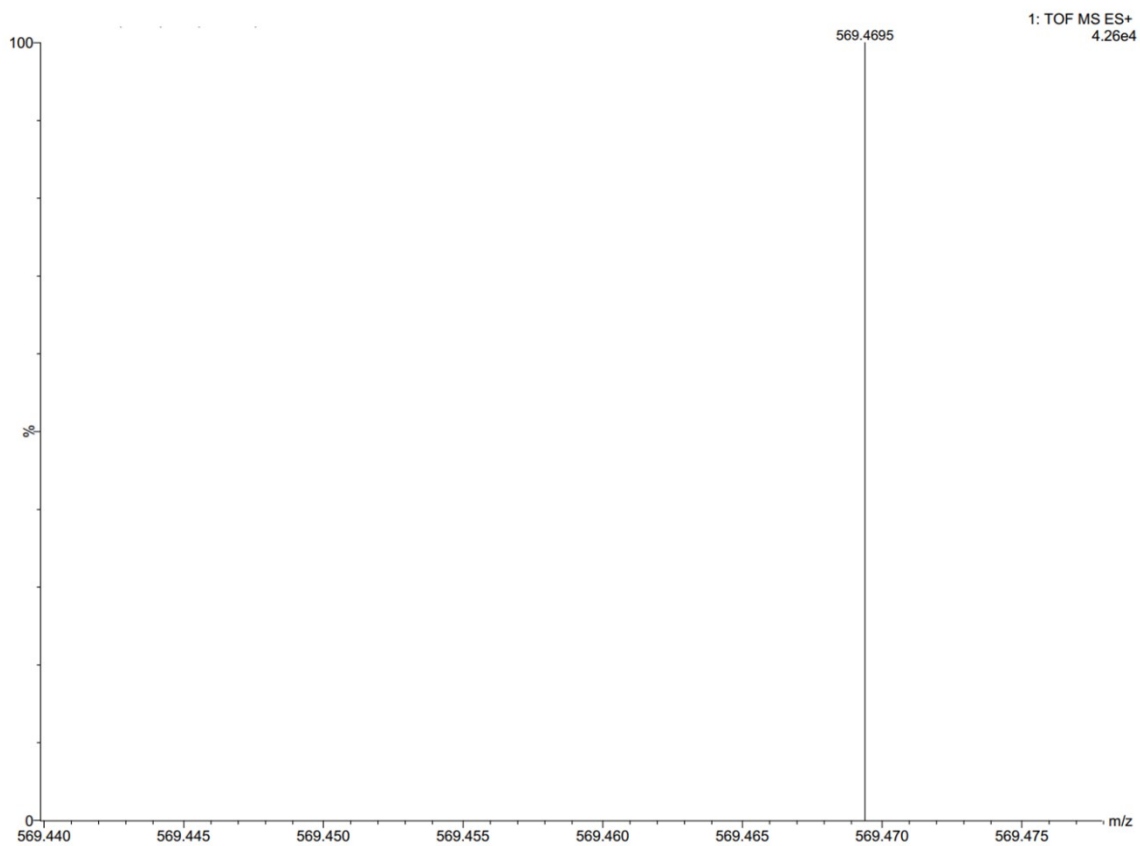

Figure S11. The ^{13}C NMR spectrum of **EAPV12**.

17
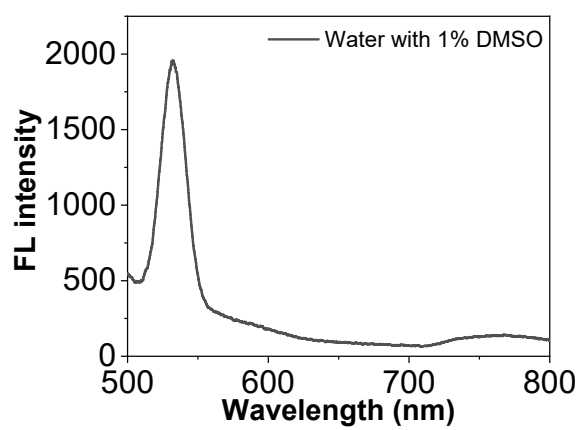
Figure S12. ESI-Mass spectrum of **EAPV12**.

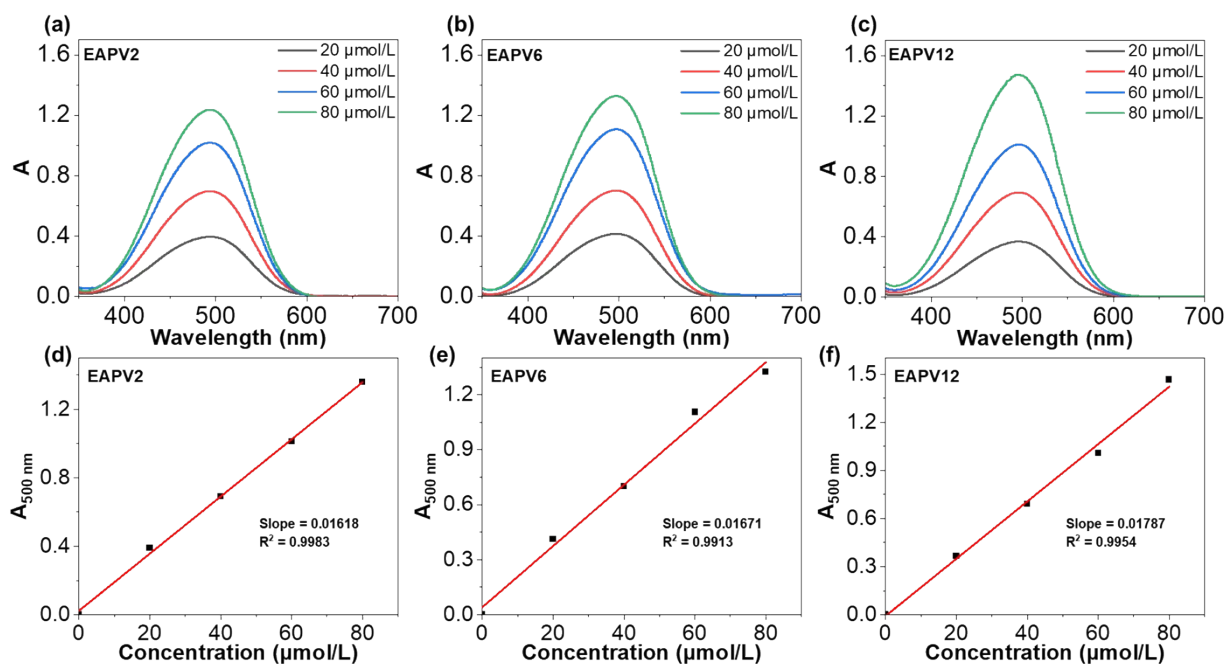Figure S13. Fluorescence spectra of water with 1% DMSO.

Figure S14. The abdorbance of a)EAPV2, b) EAPV6 and c) EAPV12 in DMSO with different concentration. The plot of absorbance at 500nm of d)EAPV2, e) EAPV6 and f) EAPV12 versus solution concentration.
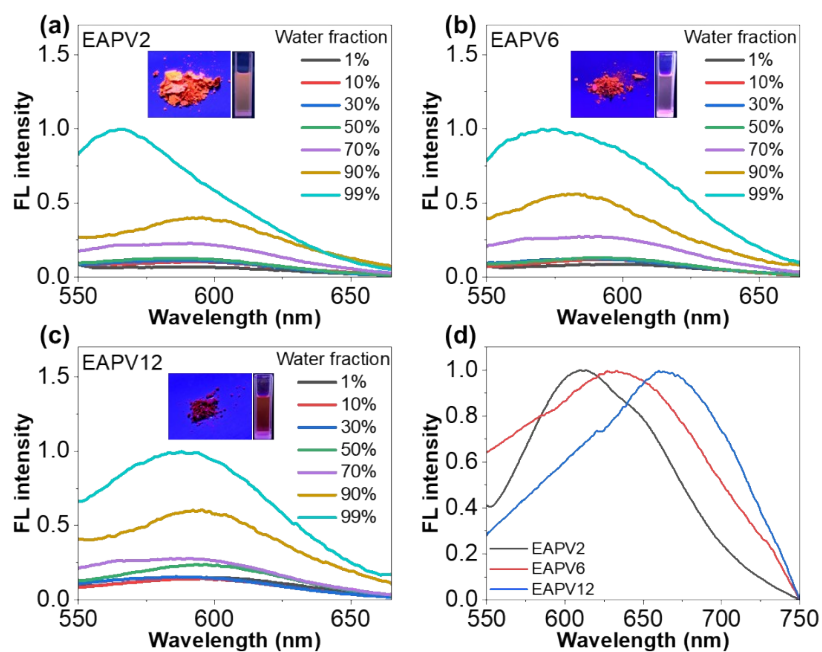

Figure S15. The fluorescence spectra of a) **EAPV2**, b) **EAPV6**, and c) **EAPV12** in a water/THF mixture with different water volume fractions from 1% to 99% (λ_{ex} = 500 nm). The

insets show the pictures of EAPVs in solid state(left) and aggregation state (right) upon Ulta-violet light irradation. d) The emission spectra of EAPVs in solid state(λ_{ex} = 500 nm).

Table S1. PLQY values of **EAPV2**, **EAPV6** and **EAPV12** in solution, aggregation state and solid state.

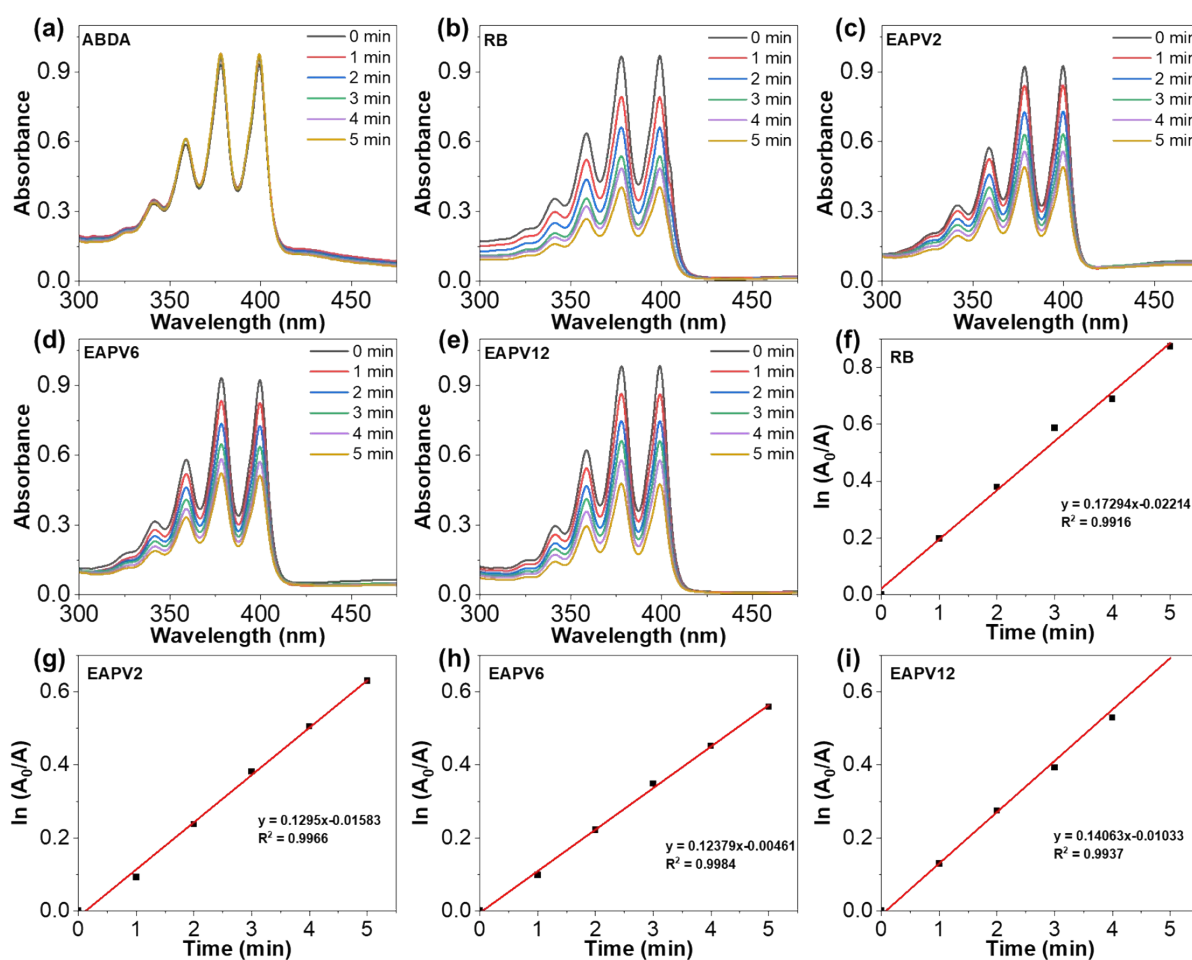| Compound	Φsolution	Φaggregation	Φsolid
EAPV2	0.02%	10.71%	16.78%
EAPV6	0.02%	11.17%	10.69%
EAPV12	0.03%	11.87%	7.19%

Figure S16. The time dependent absorbance of ABDA recorded under an white light irradiation (50 mW cm^{-2}) in samples including different photosensitizers a) ABDA only, b) RB, c) **EAPV2**, d) **EAPV6** and e) **EAPV12**. Photosensitizer concentration = 10 μM. ABDA concentration = 100 μM. The plot of decomposition rates of ABDA versus irradiation time in the presence of different photosensitizers f) RB, g) **EAPV2**, h) **EAPV6** and i) **EAPV12.**
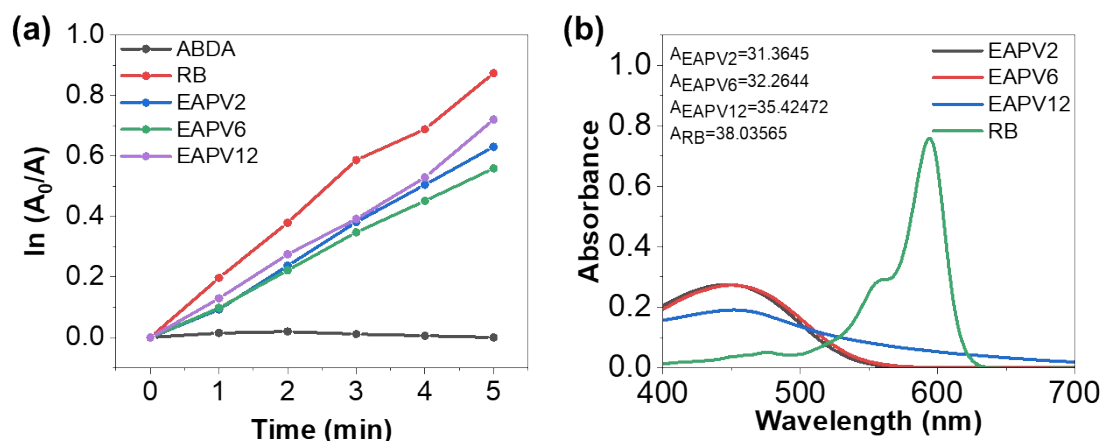

Figure S17. a) The decomposition rates of ABDA under white light irradiation (50 mW/cm^2) in the presence of different photosensitizers, where A and A$_0$ indicate the absorbance at 378 nm wavelength in the presence of ABDA with and without light irradiation, respectively. b) The UV/vis spectra of different photosensitizers, the integration of the absorbance bands at the wavelength between 400 and 700 nm (A, inside). **Table S2**. Values of the ROS quantum yield for **EAPV2**, **EAPV6** and **EAPV12** in water using RB as a standard reference.

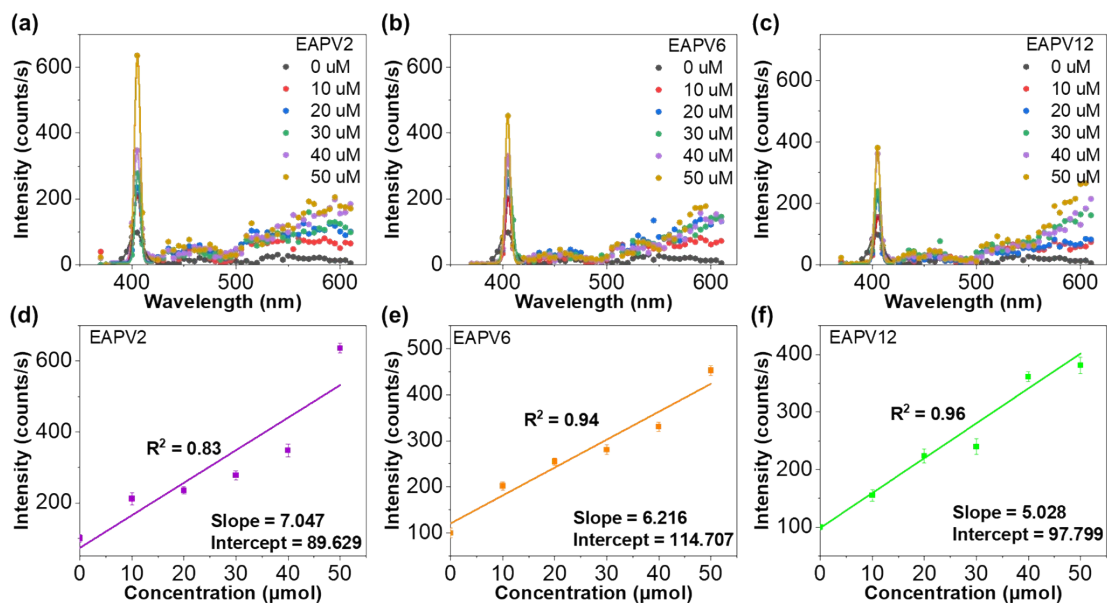| Compound	K	A	Φ
EAPV2	0.1295	31.3645	68.10%
EAPV6	0.12379	32.2644	63.28%
EAPV12	0.14063	35.4247	65.48%
RB	0.17294	38.0356	75.00%

Figure S18. Emission spectra for a) **EAPV2**, b) **EAPV6** and c) **EAPV12** in aqueous solutions with different concentrations upon excitation with femtosecond laser at 810 nm wavelength. The solid curves in a-c are the fitting of the Hyper-Rayleigh peak at 405 nm position with a Gaussian function. The linear plots in d-f are the fitted peak intensities at 405 nm with the concentration of d) **EAPV2**, e) **EAPV6** and f) **EAPV12**.
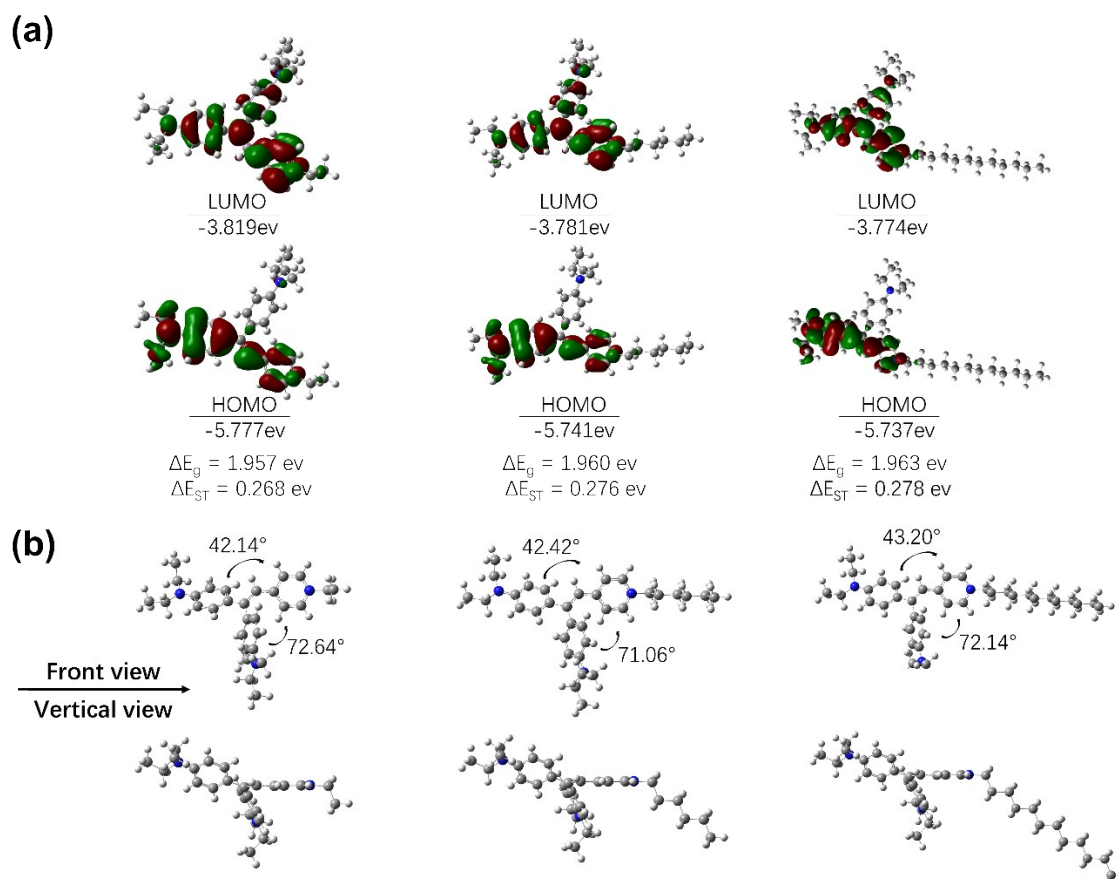
(a)

LUMO
-3.819ev

LUMO
-3.781ev

LUMO
-3.774ev

HOMO
-5.777ev

HOMO
-5.741ev

HOMO
-5.737ev

$\Delta E_g = 1.957$ ev
$\Delta E_{ST} = 0.268$ ev

$\Delta E_g = 1.960$ ev
$\Delta E_{ST} = 0.276$ ev

$\Delta E_g = 1.963$ ev
$\Delta E_{ST} = 0.278$ ev

(b)

42.14°

42.42°

43.20°

72.64°

71.06°

72.14°

Front view

Vertical view

Figure S19. a) Frontier molecular orbitals obtained from DFT calculations for **EAPV2**, **EAPV6** and **EAPV12**. b) The front and vertical views of the optimized molecular geometries in the ground state based on the B3LYP/6-31G (d) level.
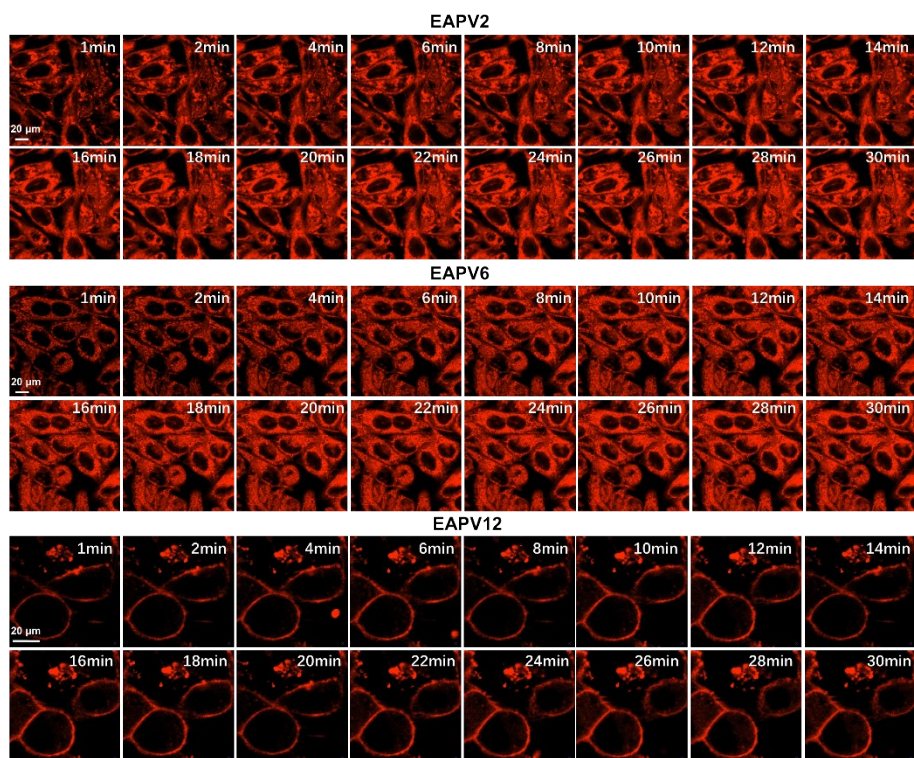
Figure S20. Time-dependent CLSM images of Hela cells labeled with **EAPVs** (E_{ex} = 500 nm, E_{em} = 580-620 nm, 20 μM).
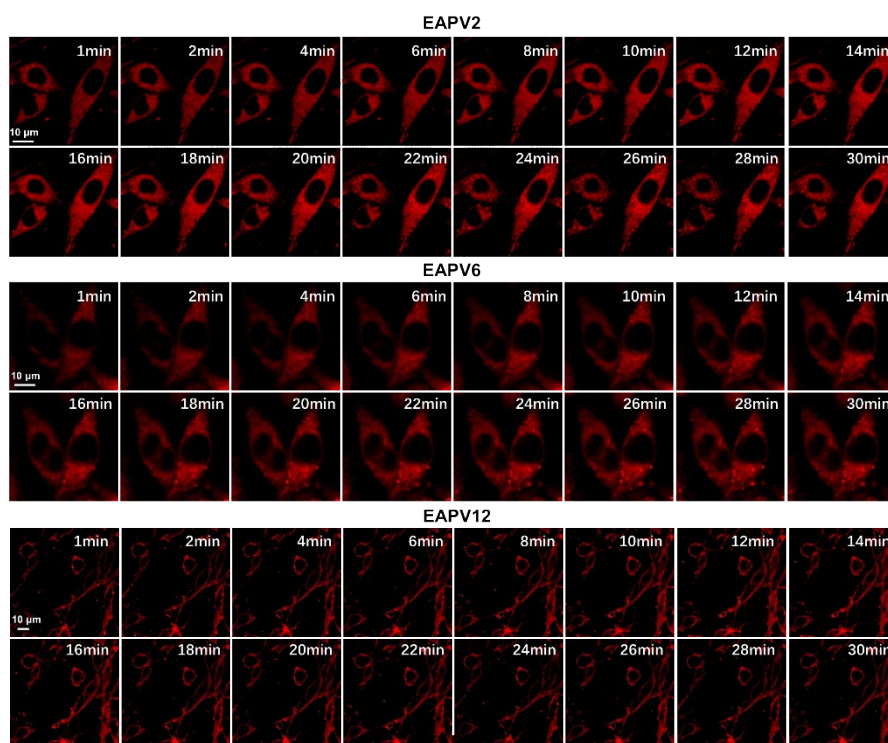
Figure S21. Time-dependent CLSM images of U87MG cells labeled with **EAPVs** (E_{ex} = 500 nm, E_{em} = 580-620 nm, 20 μM).
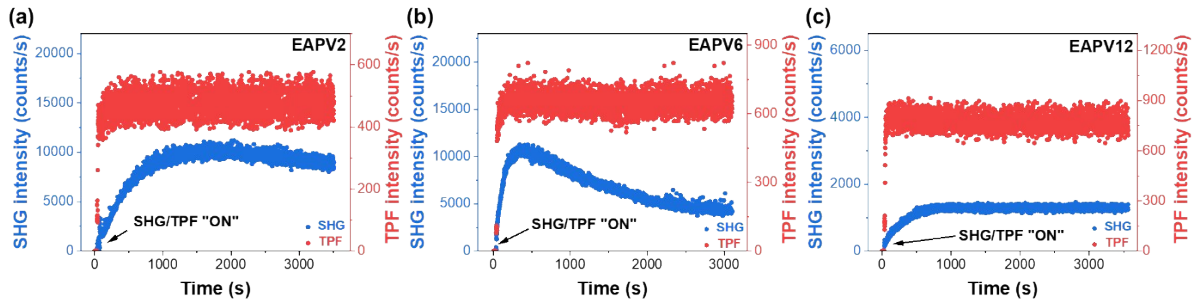
Figure S22. Time-dependent a, b, c) SHG and TPF intensities obtained from **EAPVs** (20 μM) after the addition of Hela cells upon femtosecond laser excitation at a power of 300 mw.
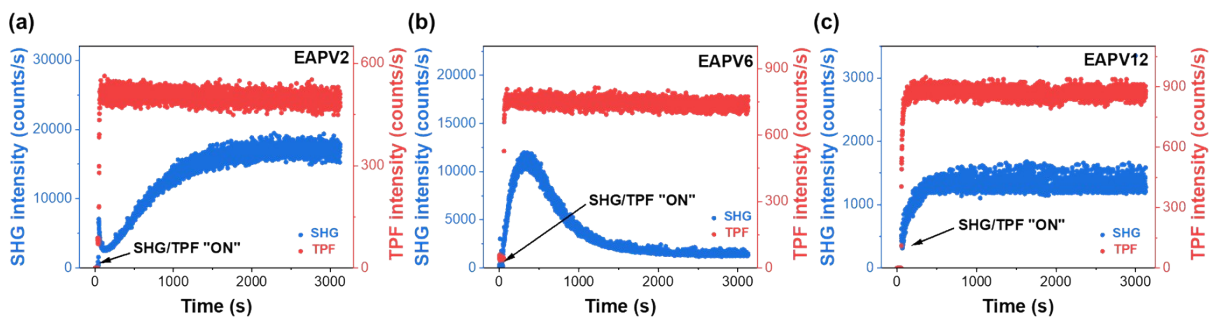

Figure S23. Time-dependent a, b, c) SHG and TPF intensities obtained from **EAPVs** (20 μM) after the addition of U87MG cells upon femtosecond laser excitation at a power of 300 mw.
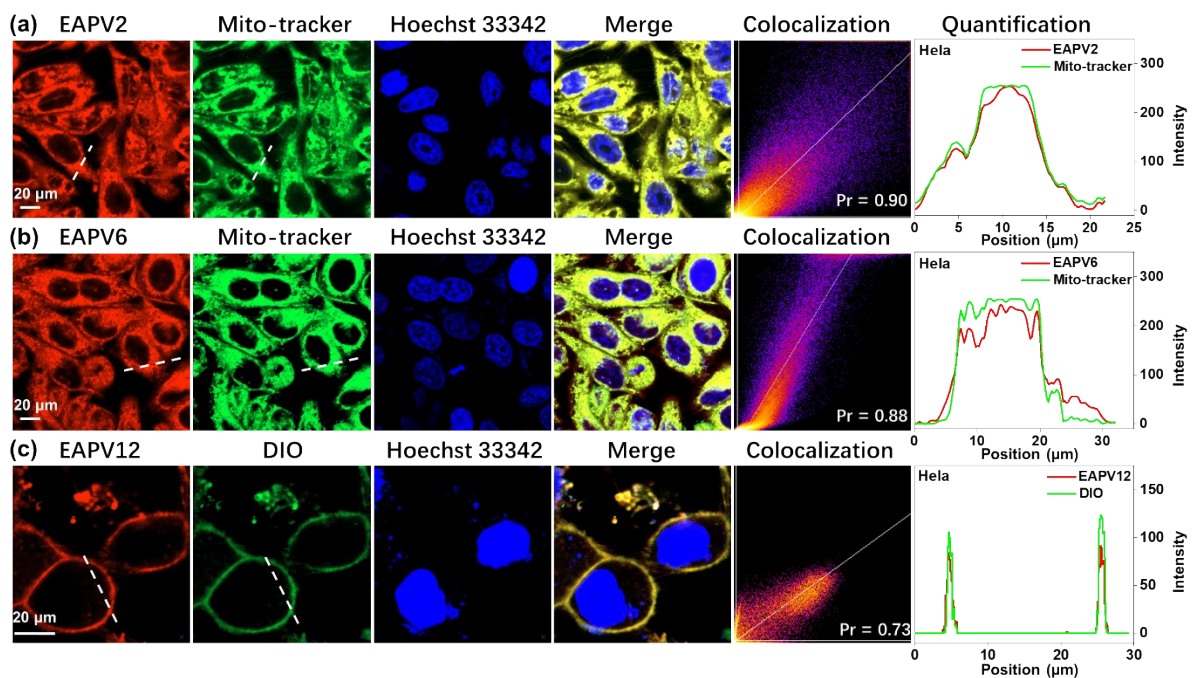
Figure S24. a, b) CLSM images of Hela cells pre-treated with Mito-tracker (green channel E_{ex} = 470 nm, E_{em} = 490-520 nm) and Hoechst 33342 (blue channel E_{ex} = 405 nm, E_{em} = 420-450 nm) co-localized with **EAPV2** and **6** for 1h (red channel E_{ex} = 500 nm, E_{em} = 580-620 nm). c) CLSM images of Hela cells pre-treated with DIO (green channel E_{ex} = 484 nm, E_{em} = 550-540 nm) and Hoechst 33342 (blue channel E_{ex} = 405 nm, E_{em} = 420-450 nm) co-localized with **EAPV 12** for 1h (red channel E_{ex} = 500 nm, E_{em} = 580-620 nm). Pr in colocalization frames indicates the Pearson's co-localization coefficient. The plot profile in quantification frames exhibit the fluorescence intensities along the white dash line marked in the **EAPVs** (red channel) and organelle-trackers (green channel), respectively.
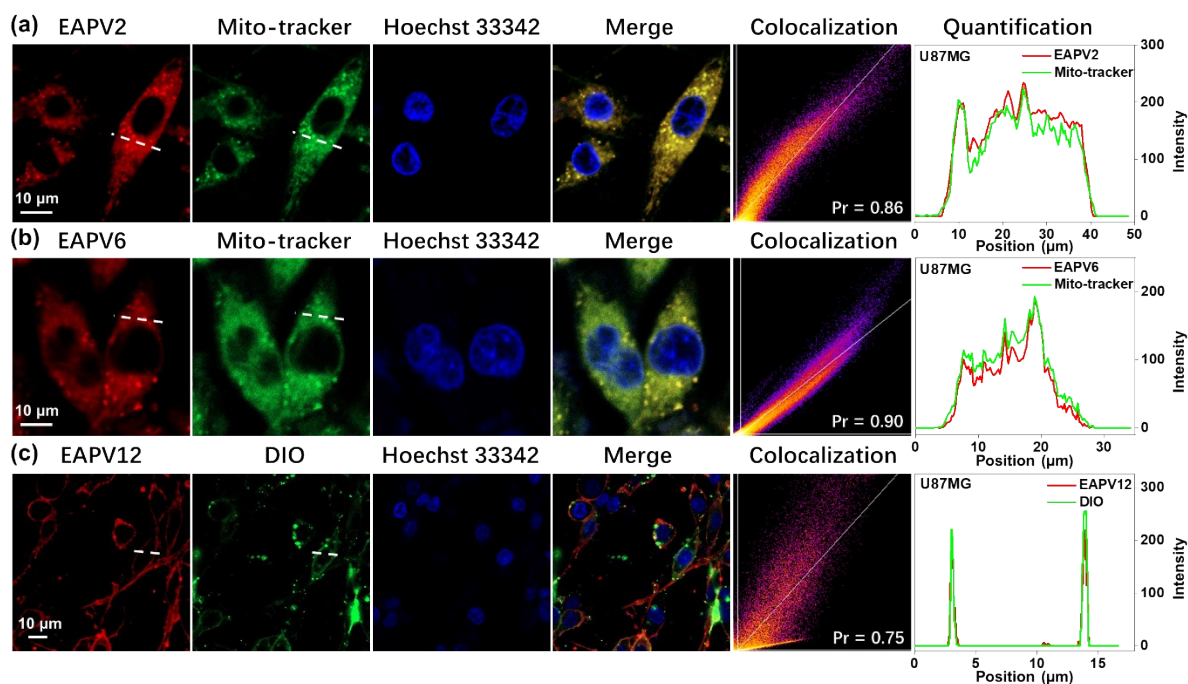

Figure S25. a, b) CLSM images of U87MG cells pre-treated with Mito-tracker (green channel E_{ex} = 470 nm, E_{em} = 490-520 nm) and Hoechst 33342 (blue channel E_{ex} = 405 nm, E_{em} = 420-450 nm) co-localized with **EAPV2** and **6** for 1h (red channel E_{ex} = 500 nm, E_{em} = 580-620 nm). c) CLSM images of U87MG cells pre-treated with DIO (green channel E_{ex} = 484 nm, E_{em} = 550-540 nm) and Hoechst 33342 (blue channel E_{ex} = 405 nm, E_{em} = 420-450 nm) co-localized with **EAPV 12** for 1h (red channel E_{ex} = 500 nm, E_{em} = 580-620 nm). Pr in colocalization

frames indicates the Pearson's co-localization coefficient. The plot profile in quantification frames exhibit the fluorescence intensities along the white dash line marked in the **EAPVs** (red channel) and organelle-trackers (green channel), respectively.
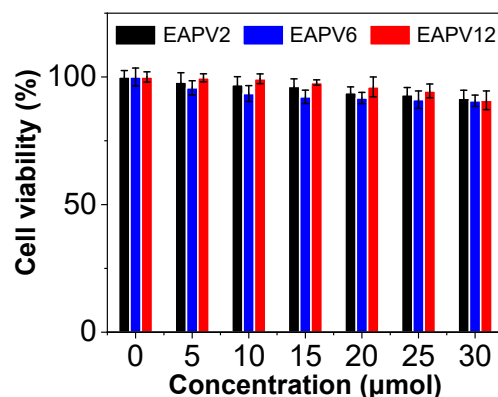

Figure S26. Viabilities of Hela cells treated with different concentration of **EAPV2**, **EAPV6**, and **EAPV12** (0 -30 μM) 24 h.

References

1. H. Xie, W. Hu, F. Zhang, C. Zhao, T. Peng, C. Zhu and J. Xu, AIE-active polyelectrolyte based photosensitizers: the effects of structure on antibiotic-resistant bacterial sensing and killing and pollutant decomposition, J. Mater. Chem. B, 2021, 9, 5309-5317.

2. Li, B.; Li, J.; Gan, W.; Tan, Y.; Yuan, Q., Unveiling the Molecular Dynamics in a Living Cell to the Subcellular Organelle Level Using Second-Harmonic Generation Spectroscopy and Microscopy. *Analytical Chemistry* **2021,** *93*, 14146-14152.

3. Li, J.; Chen, S. L.; Hou, Y.; Zhou, J.; Gan, W., Drastically modulating the structure, fluorescence, and functionality of doxorubicin in lipid membrane by interfacial density control. *The Journal of Chemical Physics* **2019,** *151*, 224706-224713.

4. Yao, C.; Chen, Y.; Zhao, M.; Wang, S.; Wu, B.; Yang, Y.; Yin, D.; Yu, P.; Zhang, H.; Zhang, F., A Bright, Renal-Clearable NIR-II Brush Macromolecular Probe with Long Blood Circulation Time for Kidney Disease Bioimaging. *Angewandte Chemie International Edition* **2022,** *61*, e202114273.